

# Kinetic study of the reactions of *tert*-butyl radicals in the liquid phase in the presence and absence of oxygen

Andrew R. Costello, John R. Lindsay Smith,\* Moray S. Stark and David J. Waddington

Department of Chemistry, University of York, Heslington, York, UK YO1 5DD

The photolyses of solutions of 2,2'-azoisobutane and 2,2,4,4-tetramethylpentan-3-one in decane in glass and metal cells, have been used to generate *tert*-butyl and, by reaction with oxygen, *tert*-butylperoxyl radicals. Time-dependent product yields from reactions in oxygenated and oxygen-free solutions have been measured over a range of temperatures (298–398 K). For each precursor, for a given set of conditions, the general features of the reactions are independent of the cell used, although the absolute rates of product formation are different. The major difference between the reactions of the two precursors lies in the initial photochemical step. For 2,2'-azoisobutane this leads directly to two *tert*-butyl radicals whereas the ketone gives a *tert*-butyl and a 2,2-dimethylpropanoyl radical. The product distributions can be accounted for in terms of the reactions of these radicals within a solvent cage in competition with cage escape and subsequent reaction. A single kinetic model that accounts for the reactions of both precursors, in the presence or absence of oxygen, at the temperatures studied, is described.

A thorough understanding of the mechanisms of autoxidation is essential for the development of oils and lubricants with improved thermo-oxidative stability, such as esters.<sup>1</sup> Unfortunately, the relevant rate constants and reactions of the radicals formed in these processes are generally not well characterised. As a consequence the development of a computer model to describe these systems suffers from large uncertainties.

In earlier studies,<sup>2,3</sup> we attempted to obtain data for simple primary and secondary alkylperoxyl radicals from the photolysis of azoalkanes. These were then modelled by kinetic simulation using the best available values or estimates for rate constants of the individual steps.

We have now extended the study in three significant ways. First, we have examined the reactions of a tertiary alkylperoxyl radical which are important since such radicals are commonly formed in the autoxidation of lubricants.<sup>1</sup> Secondly, we have extended the study to higher temperatures by using a ketone as the precursor for the peroxyl radical. Thirdly, we have studied the reaction in cells made of different materials. In this way, we are now able to define the effects of temperature, type of reaction vessel and the source of the radical on the rates of the competing radical reactions. The radical chosen is *tert*-butylperoxyl, the precursors are 2,2'-azoisobutane and 2,2,4,4-tetramethylpentan-3-one and the cells are made of Pyrex and steel. Kinetic simulation of time-dependent studies leads to a general model that accounts for the observed results.

## Experimental

### Reagents

Unless otherwise stated, all reagents were commercially available and used without further purification. The decane solvent was purified by alumina column chromatography and minor volatile impurities in the 2,2,4,4-tetramethylpentan-3-one radical precursor were removed by vacuum distillation, 37–41 °C at 25 mmHg. 2,2'-Azoisobutane was prepared from *tert*-butylamine by the method of Ohme *et al.*<sup>4</sup> and had bp 22–25 °C at 30 mmHg (lit.,<sup>4,5</sup> 108–110 °C at 760 mmHg), <sup>1</sup>H NMR  $\delta$  1.17 and <sup>13</sup>C NMR  $\delta$  29.57 and 70.61; *m/z* 142(M<sup>+</sup> 0.3%), 57(100), 41(47), 71(8), 127(0.5) and 85(0.3).

### Analytical methods

GC analysis of reaction mixtures involved two columns and analyses were run simultaneously using Pye Unicam GCD and PU4500 gas chromatographs, each fitted with a flame ionisation detector. For reactions using 2,2,4,4-tetramethylpentan-3-one, 20%(w/w) dinonyl phthalate on Gas Chrom Q was employed as the packing material to quantify the *tert*-butanol, 2,2,3,3-tetramethylbutane and di-*tert*-butyl peroxide and silica gel for analysis of the hydrocarbons. For the 2,2'-azoisobutane reactions the former column was replaced by one containing Porapak T. Data collection and analysis used a Trivector Trio data station.

The concentration of oxygen in oxygen-saturated decane at different temperatures was measured using a Pye 104 gas chromatograph equipped with a thermal conductivity detector. This required two packed columns connected in series; the first, which contained silica gel, was used to retain decane, and the second was fitted with molecular sieve 5A. The first column was periodically disconnected and regenerated by purging the adsorbed decane with nitrogen at 200 °C. The system was calibrated with gaseous oxygen-nitrogen mixtures prepared on a vacuum line.

Two methods were used to attempt to quantify hydrogen peroxide and hydroperoxides. The first, which involved iodometric titrations of aqueous extracts of reaction mixtures, could not be used for reactions with the ketone precursor since the latter compound interfered with the analysis.<sup>6</sup> The second, which used horseradish peroxidase to quantify hydrogen peroxide and hydroperoxides and horseradish peroxidase with catalase to estimate alkyl hydroperoxides,<sup>7,8</sup> proved to be too insensitive to *tert*-butyl hydroperoxide.

Formaldehyde in aqueous extracts of reaction mixtures was determined by the Nash test.<sup>9</sup>

### Reaction cells

The design of the glass cell with a Pyrex optical window has been described previously.<sup>2</sup> The metal cell consisted of a stainless-steel tube with three side arms and Pyrex optical windows attached at each end with teflon O-rings and screw-on caps. One side arm, sealed with a septum, was used to extract samples with a syringe for GC analysis. The other two were designed to attach the cell to a vacuum-line system. The

temperature in the cell was maintained with an electrically heated aluminium heating jacket. The temperature was monitored and controlled by a thermocouple connected to an electroserv control unit. Solutions inside the cells were stirred using a small magnetic follower.

Both cells were constructed so that they could be completely filled with liquid to prevent the escape of volatile products into a gas head-space.

Light source

Photolysis was by a high-pressure mercury lamp (HBO 200 W/4 Wotan type) contained in a ventilated steel housing, fitted with a shutter. The output of the lamp was focussed with lenses onto the reaction cell.

The constancy of the output of the lamp was checked by measuring the rate of formation of products from the photolysis of the azo or ketone precursors in absence of oxygen.

Photolysis procedure

Decane, which had been thoroughly saturated with either nitrogen or oxygen, was introduced into the reaction cell and the required amount of azo or ketone precursor added. The reaction solution was stirred and allowed to equilibrate to the required temperature before photolysis was initiated. After the required time photolysis was stopped and the reaction mixture was analysed by GC.

Computer simulation

The program used in this work, SIMULA, was originally written and donated by A. Prothero (Shell Research Ltd) and was further modified to allow experimental data to be compared graphically with the simulated results.<sup>10,11</sup>

Results

Photolysis of 2,2,4,4-tetramethylpentan-3-one and 2,2'-azoisobutane in decane

The anaerobic photolysis of 2,2,4,4-tetramethylpentan-3-one, between 323 and 373 K, and of 2,2'-azoisobutane, between 323 and 348 K, in decane, has been studied in a metal cell (Table 1). The only products detected were 2-methylpropane, 2-methylpropene and 2,2,3,3-tetramethylbutane, the increase in yield of all three being more-or-less linear with time.

On increasing the temperature for both reactants, the rate of 2-methylpropane formation increases with respect to those

of 2-methylpropene and 2,2,3,3-tetramethylbutane and, in turn, the rate of formation of 2-methylpropene decreases relative to that of 2,2,3,3-tetramethylbutane.

Photo-oxidation of 2,2,4,4-tetramethylpentan-3-one in decane

The photolysis of 2,2,4,4-tetramethylpentan-3-one in oxygenated decane was studied between 323 and 398 K in a metal cell (Table 2) and between 298 and 348 K in a glass cell (Table 3). The major products detected at all temperatures were 2-methylpropane, 2-methylpropene, *tert*-butanol, 2,2,3,3-tetramethylbutane and di-*tert*-butyl peroxide. The general features of the results from the experiments using both cells and at all temperatures were similar although the absolute rates were found to be different. Thus only those obtained at 323 K in the metal cell will be described in detail (Fig. 1, Table 2).

The only products detectable initially are 2-methylpropene and *tert*-butanol, together with trace amounts of di-*tert*-butyl peroxide. The rate of production of *tert*-butanol is initially large and then the yield levels to a constant value. The rate of production of 2-methylpropene during this initial period is much lower but coincident with the levelling-off of *tert*-butanol, there is a large increase in rate, and 2-methylpropane and 2,2,3,3-tetramethylbutane are also formed. All three hydrocarbon products show subsequent growth that is roughly linear with time. The concentration of di-*tert*-butyl peroxide also increases significantly at this point in the reaction before levelling off.

As the temperature is increased, although the rate of formation of *tert*-butanol increases, its final concentration is lower. The growth of 2-methylpropene decreases with increasing temperature in the initial phase of the reaction such that at 373 and 398 K only trace amounts are detected during this period. Furthermore, the rate of production of 2-methylpropene and 2,2,3,3-tetramethylbutane in the second phase of reaction also decrease with increasing temperature. Conversely, the relative rate of formation of 2-methylpropane compared to that of 2-methylpropene shows a marked increase with respect to temperature.

Photo-oxidation of 2,2'-azoisobutane in decane

The photolysis of 2,2'-azoisobutane in oxygen-saturated decane was studied in the metal cell at 323 and 348 K and in the glass cell at 298, 323 and 348 K (Table 4). The major products detected at all temperatures were 2-methylpropane, 2-methylpropene, *tert*-butanol and 2,2,3,3-tetramethylbutane. The general features of the results from all the experiments at all the temperatures studied were the same and only those

Table 1 Photolysis of 2,2,4,4-tetramethylpentan-3-one (KET) and 2,2'-azoisobutane (AZO) in decane in a metal cell

reactant	temperature /K	photolysis time/s	concentration/10 <sup>-4</sup> mol dm <sup>-3</sup>			
			C <sub>4</sub> H <sub>10</sub>	C <sub>4</sub> H <sub>8</sub>	C <sub>8</sub> H <sub>18</sub>	Bu <sub>tot</sub>
KET	323	180	3.4	2.4	0.4	6.6
		1080	14.7	9.8	1.2	26.9
		4680	70.5	53.0	7.4	138.3
		1080	15.1	10.8	—	—
	348	2880	35.8	19.3	2.9	60.9
		4680	57.0	31.8	5.4	100.6
		720	10.0	4.9	0.5	15.9
	373	2520	40.8	16.8	2.8	63.6
		4680	79.5	33.5	4.4	121.8
AZO	323	300	3.2	3.1	0.3	6.9
		900	13.6	11.2	1.8	28.4
		1800	28.7	21.9	3.7	58.0
		300	4.2	3.6	0.4	8.6
	348	900	14.8	10.9	1.9	29.5
		1800	30.2	22.5	3.9	60.5

Initial concentrations of KET and AZO, 2.7 × 10<sup>-2</sup> mol dm<sup>-3</sup>. Bu<sub>tot</sub> refers to the total concentration of *tert*-butyl radicals that form products.

Table 2 Photo-oxidation of KET in decane in a metal cell

T/K	oxygen conc. /10 <sup>-3</sup> mol dm <sup>-3</sup>	photolysis time/s	concentration/10 <sup>-4</sup> mol dm <sup>-3</sup>							
			C <sub>4</sub> H <sub>10</sub>	C <sub>4</sub> H <sub>8</sub>	C <sub>8</sub> H <sub>18</sub>	C <sub>4</sub> H <sub>9</sub> OH	C <sub>4</sub> H <sub>9</sub> OOC <sub>4</sub> H <sub>9</sub>	Bu <sub>HC</sub>	Bu <sub>ox</sub>	Bu <sub>tot</sub>
323	5.6	300	0.15	0.5	0	5.0	0.2	0.65	5.4	6.0
		600	0.01	0.9	0	8.8	0.2	0.91	9.2	10.1
		900	0.18	1.2	0	13.8	0.5	1.4	14.8	16.2
		1200	0.04	2.0	0	14.8	0.4	2.0	15.6	17.6
		1500	0.55	5.7	0.9	28.0	0.2	8.0	28.4	36.4
		1800	10.3	10.3	1.3	27.1	1.3	23.2	29.7	52.9
		2100	15.1	11.6	2.0	29.0	2.7	30.7	34.4	65.1
		2700	21.6	14.4	3.0	28.6	2.6	42.0	33.8	75.8
		3600	50.5	47.6	4.0	37.6	13.9	106.1	65.4	171.5
		3600	47.8	42.2	4.0	34.1	15.9	98.0	65.9	163.9
		5400	71.2	63.0	7.2	29.3	15.3	148.6	59.9	208.5
		7200	91.0	77.0	10.5	32.2	15.5	189.0	63.2	252.2
348	4.8	900	0.9	1.1	0	11.3	0.2	2.0	11.8	13.8
		1800	13.6	9.8	1.0	13.6	1.3	25.4	16.2	41.6
		1800	13.5	9.5	1.0	19.4	3.3	25.0	26.0	51.0
		3600	25.4	18.0	3.3	17.8	2.8	50.0	23.4	73.4
		3600	26.8	17.8	3.3	14.3	3.2	51.2	20.7	71.9
		5400	47.7	35.0	5.6	16.4	7.4	93.9	31.2	125.1
		5400	48.9	34.4	5.6	16.9	5.8	94.5	28.5	123.0
		7200	66.7	47.8	8.0	17.4	6.5	130.5	30.4	160.9
373	4.3	600	0.3	0.1	0	5.6	0.6	0.4	6.8	7.2
		900	0.7	0.4	0	6.3	0.4	1.1	7.1	8.2
		900	1.0	0.3	0	11.0	0.3	1.3	11.6	12.9
		1200	0.8	0.4	0	16.5	0.4	1.2	17.3	18.5
		1500	5.8	3.0	0.4	10.2	1.6	9.6	13.4	23.0
		2100	14.6	4.6	1.1	15.0	2.0	21.4	19.0	40.4
		2700	24.4	7.0	2.0	16.5	1.8	35.4	20.1	55.5
		5400	60.2	23.0	5.0	19.5	2.1	93.2	23.7	116.9
398	3.4	600	0.9	0.3	0	6.9	0	1.2	6.9	8.1
		900	0.9	0.4	0	9.0	0	1.3	9.0	10.3
		1200	6.3	2.6	0	8.3	0	8.9	8.3	17.2
		1800	11.6	2.9	0.9	7.0	0	16.3	7.0	23.3
		3600	48.9	9.4	3.5	8.9	0	65.3	8.9	74.2

Initial concentration of KET = 2.7 × 10<sup>-2</sup> mol dm<sup>-3</sup>. Bu<sub>HC</sub>, Bu<sub>ox</sub>, Bu<sub>tot</sub> refer to the concentrations of *tert*-butyl radicals which form hydrocarbon, oxygenated and total products.

obtained at 323 K in the metal cell are described in detail (Fig. 2).

In the initial phase, the rate of growth of the four products is approximately constant. Then, after a period of time, which is dependent on the temperature, the rate of growth of *tert*-butanol begins to decrease. At the higher temperatures studied,

there is an increase in the rate of growth of each of the three hydrocarbon products as the concentration of *tert*-butanol comes to a maximum.

As with the results obtained for the photo-oxidation of 2,2,4,4-tetramethylpentan-3-one, the only marked difference between the two cells is the absolute rate of product forma-

Table 3 Photo-oxidation of KET in decane in a glass cell

T/K	oxygen conc. /10 <sup>-3</sup> mol dm <sup>-3</sup>	photolysis time/s	concentration/10 <sup>-4</sup> mol dm <sup>-3</sup>							
			C <sub>4</sub> H <sub>10</sub>	C <sub>4</sub> H <sub>8</sub>	C <sub>8</sub> H <sub>18</sub>	C <sub>4</sub> H <sub>9</sub> OH	C <sub>4</sub> H <sub>9</sub> OOC <sub>4</sub> H <sub>9</sub>	Bu <sub>HC</sub>	Bu <sub>ox</sub>	Bu <sub>tot</sub>
298	6.1	1800	0.1	0.4	0	18.9	0.3	0.5	19.4	19.9
		3600	6.4	7.4	1.2	42.9	1.6	16.2	46.1	62.3
		3600	6.5	10.7	1.2	41.6	1.8	19.6	45.2	64.8
		5400	28.3	21.3	2.4	37.4	6.3	54.4	50.0	104.4
		7200	44.3	30.0	3.5	40.1	9.0	81.3	58.1	139.4
		7200	42.2	30.2	3.5	41.3	7.8	79.4	56.9	136.3
		12300	100.5	68.5	7.0	43.9	15.0	183.0	73.9	256.9
323	5.6	600	0.02	0.5	0	5.9	0	0.5	5.9	6.4
		1800	0.1	1.4	0	9.4	0.12	1.5	9.6	11.1
		1800	0.1	1.0	0	7.5	0.45	1.1	8.4	9.5
		3600	12.8	8.6	0.8	21.3	3.9	23.0	29.1	52.1
		3600	9.8	6.3	0.8	28.5	2.8	17.7	34.1	51.8
		4500	15.5	9.5	1.6	36.4	3.2	27.2	42.8	70.0
		5400	29.7	19.5	2.0	30.0	6.7	53.2	43.4	96.6
		5400	27.0	14.0	2.0	31.7	7.9	45.0	47.5	92.3
		7200	35.2	23.6	3.2	24.8	7.3	65.2	39.1	104.3
		7200	40.0	26.0	3.2	25.5	7.3	72.4	40.1	112.5
		900	0.02	0.3	0	10.6	0.4	0.3	11.4	11.7
		1800	4.2	3.2	0.5	22.8	1.2	8.4	25.2	33.6
348	4.8	3600	31.7	19.2	2.3	15.4	5.2	55.5	25.8	81.3
		5400	42.9	25.4	4.2	21.7	6.3	76.7	34.3	111.0
		7200	59.7	33.6	6.2	14.6	8.4	105.7	31.4	137.1

Initial concentration of KET = 2.7 × 10<sup>-2</sup> mol dm<sup>-3</sup>. Bu<sub>HC</sub>, Bu<sub>ox</sub>, Bu<sub>tot</sub> refer to the concentrations of *tert*-butyl radicals which form hydrocarbons, oxygenated and total products.

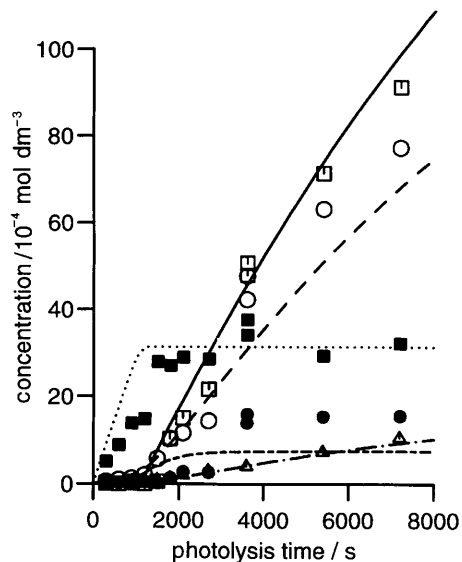


**Fig. 1** Photo-oxidation of 2,2,4,4-tetramethylpentan-3-one in decane in a metal cell. Experimental data at 323 K. Ketone  $2.7 \times 10^{-2}$  mol dm $^{-3}$ ; oxygen  $5.6 \times 10^{-3}$  mol dm $^{-3}$ . Symbols are experimental results, lines are simulated results:  $\square$ , (—) 2-methylpropane;  $\circ$ , (—) 2-methylpropene;  $\triangle$ , (—) 2,2,3,3-tetramethylbutane;  $\blacksquare$ , (—) *tert*-butanol;  $\bullet$ , (—) di-*tert*-butyl peroxide.

tion, the relative rates being fairly similar for a given temperature. In both cells the initial rate of *tert*-butanol formation is virtually identical at all temperatures studied; as the temperature is increased, the final concentration of *tert*-butanol is lower.

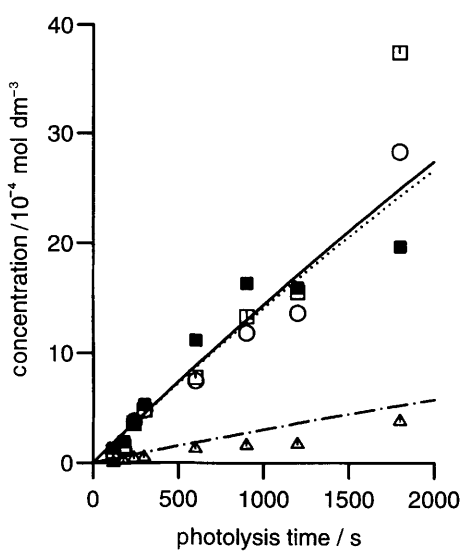


**Fig. 2** Photo-oxidation of 2,2'-azoisobutane in decane in a metal cell. Experimental data at 323 K. Azo compound  $2.7 \times 10^{-2}$  mol dm $^{-3}$ ; oxygen  $5.6 \times 10^{-3}$  mol dm $^{-3}$ . See Fig. 1 for key.

The initial concentrations of oxygen in the photo-oxidation mixtures, at the temperatures used in this study, were measured by gas chromatography. As expected the values decrease with increasing temperature.

Discussion

The relative rates of formation of products change on altering the precursor from 2,2'-azoisobutane to 2,2,4,4-

**Table 4** Photo-oxidation of AZO in decane in metal (M) or glass (G) cells

T/K	oxygen conc. /10 $^{-3}$ mol dm $^{-3}$	photolysis time/s	concentration/10 $^{-4}$ mol dm $^{-3}$					
			C $_4$ H $_{10}$	C $_4$ H $_8$	C $_8$ H $_{18}$	C $_4$ H $_9$ OH	Bu $_{HC}$	Bu $_{tot}$
323 (M)	5.6	120	1.0	0.7	0	1.3	1.7	3.0
		180	1.5	1.2	0.2	1.9	3.1	5.0
		240	3.6	3.8	0.4	3.8	8.2	12.0
		300	4.8	4.8	0.5	5.3	10.6	15.9
		600	7.8	7.5	1.3	11.2	17.9	29.1
		900	13.4	11.9	1.6	16.4	28.4	44.8
		1200	15.6	13.7	1.7	16.0	32.7	48.7
		1800	37.4	28.3	3.8	19.7	73.3	93.0
348 (M)	4.8	120	2.0	1.5	0.1	3.0	3.7	6.7
		180	3.0	1.7	0.4	4.5	5.5	10.0
		240	4.0	3.0	0.3	4.0	7.6	11.6
		300	4.5	3.7	0.4	4.5	9.0	13.5
		600	10.7	9.6	1.2	12.4	22.7	35.1
		900	14.1	13.1	3.5	15.2	34.2	49.4
		1800	46.1	33.6	4.6	23.6	88.9	112.5
		1800	46.1	33.6	4.6	23.6	88.9	112.5
298 (G)	6.1	120	4.8	4.8	0.5	5.6	10.6	16.2
		240	9.9	9.9	1.3	8.4	22.4	30.8
		300	12.5	12.3	1.7	10.7	28.2	38.9
		1080	21.7	19.2	2.5	19.6	45.9	65.5
		1480	52.5	47.0	6.6	39.0	112.7	151.7
		1680	88.0	77.5	9.8	53.0	185.1	238.1
		1800	88.0	77.5	9.8	53.0	185.1	238.1
		1800	88.0	77.5	9.8	53.0	185.1	238.1
323 (G)	5.6	180	5.0	4.1	0.8	6.4	10.7	17.1
		240	6.5	5.3	1.1	8.6	14.0	22.6
		300	7.7	7.1	1.3	7.6	17.4	25.0
		600	18.1	16.1	2.6	23.8	39.4	63.2
		1200	59.0	46.9	8.1	34.7	122.1	156.8
		1800	85.5	66.8	10.4	37.4	173.1	210.5
		1800	85.5	66.8	10.4	37.4	173.1	210.5
		1800	85.5	66.8	10.4	37.4	173.1	210.5
348 (G)	4.8	120	2.5	2.3	0.3	4.1	5.4	9.5
		180	4.3	3.9	0.4	7.8	9.0	16.6
		240	5.8	5.3	0.6	9.9	12.3	22.2
		300	6.1	5.5	0.7	12.6	13.0	25.6
		600	22.7	17.4	2.9	26.5	45.9	72.4
		1200	69.2	49.8	8.0	26.7	135.0	161.7
		1800	98.8	82.5	13.5	32.9	208.0	240.9
		1800	98.8	82.5	13.5	32.9	208.0	240.9

Initial concentration of AZO =  $2.7 \times 10^{-2}$  mol dm $^{-3}$ . Bu $_{HC}$  and Bu $_{tot}$  refer to the concentration of *tert*-butyl radicals which form hydrocarbon and total products, respectively.



tetramethylpentan-3-one. They also change on raising the temperature. However, although the absolute rates of formation of products change on altering the cell, using steel instead of Pyrex, the relative rates are more-or-less constant, showing that the changes in absolute values are a function of the cell design and consequently the rate of photolysis of the substrate.

The discussion below is structured in terms of the various radical processes in the reaction.

### Initiation reactions

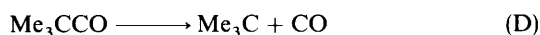
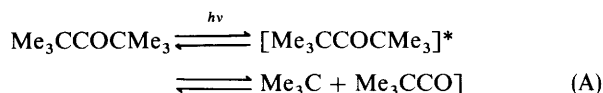
One of the key differences between the photo-oxidation of 2,2,4,4-tetramethylpentan-3-one and that of 2,2'-azoisobutane in decane is the amount of hydrocarbon products formed initially. With 2,2,4,4-tetramethylpentan-3-one virtually all the initial products are oxygenated, whereas with 2,2'-azoisobutane, hydrocarbons account for between 50 and 60% of the initial products.

The liquid phase photo-oxidation of azoethane and of 2,2'-azopropane also leads to a high proportion of hydrocarbons in the initial stages of the reaction.<sup>3,12</sup> Conversely, no hydrocarbons are amongst the products in the initial stages of the gas-phase photo-oxidation of 2,2'-azopropane.<sup>13–15</sup>

The mechanism of photolysis of azo compounds has been extensively studied.<sup>16</sup> Following the initial photo-excitation, two reactions can occur, carbon–nitrogen bond cleavage and isomerisation of the *trans* to the less stable *cis* compound. The *cis*-isomer of tertiary azo compounds is thermally labile and readily decomposes at room temperature and the latter reaction may be the predominant route for the production of alkyl radicals. However, whether the carbon–nitrogen bond cleavage occurs directly or *via* the *cis*-isomer, or both, a rate constant can be calculated for the net rate of formation of alkyl radicals in a solvent cage. In turn, the formation of hydrocarbon products from the start of the reaction can be accounted for by the initial formation of radicals in the solvent cage. This has the effect of increasing the chance of the radicals reacting with each other before they enter the bulk of the solution and react with oxygen. In the gas phase no such holding together of the radicals occurs and they separate rapidly on photolysis, to yield two discrete radicals which then undergo the more kinetically favourable reaction with oxygen.<sup>17</sup>

The proportion of radical–radical reactions that occur in the cage depends on the nature of the azo compound, the solvent and the temperature. Although the nitrogen molecule between the radicals in the solvent cage hinders the self-reaction, the radicals are still able to react together under all conditions studied.<sup>18</sup>

In contrast, the photolysis of 2,2,4,4-tetramethylpentan-3-one under the conditions of these experiments is believed to be a stepwise process resulting in an alkyl and acyl radical pair [reaction (A)] rather than the direct formation of two alkyl radicals and carbon monoxide:



The radicals are held in a solvent cage [reaction (A)] but cage reaction at this point will result in either regeneration of the starting material or disproportionation to 2,2-dimethylpropanal and 2-methylpropene [reaction (B)]. Evidence for this stepwise mechanism is supported by, first, the detection of this aldehyde product in the low-temperature photolysis of the ketone.<sup>19</sup> Secondly, with photolyses in the presence of radical

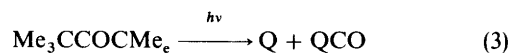
scavengers all the *tert*-butyl radicals were scavenged, demonstrating that the two primary radicals diffuse apart before decarbonylation of the acyl radical [reaction (D)].<sup>20</sup> If decarbonylation had occurred in the initial cage, then at the concentrations of scavenger used in the experiment any subsequent self-reaction of the two *tert*-butyl radicals in the cage would not have been prevented by the scavenger. Furthermore, by measuring the quantum yield of geminate recombination, it was shown that the amount of cage reaction for 2,2,4,4-tetramethylpentan-3-one is much lower than for 2,2'-azoisobutane.<sup>20</sup> The difference was attributed to the triplet character of the primary radical pair produced from the excited ketone triplet, where spin inversion of one of the radicals is necessary before cage reaction can occur<sup>21</sup> and, in contrast to the process with the azo compound, cage escape and subsequent reaction of the radicals with oxygen in the solvent is favoured.

### Assumptions of the kinetic model

The aim of this study was to develop a unified kinetic model of the photolyses and photo-oxidations of 2,2'-azoisobutane and 2,2,4,4-tetramethylpentan-3-one which would provide a quantitative description of the measured time and temperature dependence of the product distributions. Where reliable literature kinetic data on individual steps are available, these have been incorporated into the model, other rate constants are a best approximation using values from analogous or related reactions.

As described above, for each precursor the initial photochemical step generates a pair of radicals within a solvent cage. In the kinetic model we have assumed that, within this cage, the radicals only react with each other. As a corollary, after cage escape, the self-reactions of these primary radicals are relatively unimportant compared with their reactions with other molecules, *e.g.* solvent and oxygen.

To simulate the reactions, a simpler scheme for the initiation reactions was used (Appendix I) in which the net rate of caged radicals described above as reaction (A) becomes



where Q and QCO are the 'caged' radicals  $\text{Me}_3\text{C}$  and  $\text{Me}_3\text{CCO}$ . The net rate of forming free (*i.e.* non-caged) radicals, reactions A and C was expressed as:



To simplify the modelling to enable the simulation to distinguish between the two types of radicals, we have treated the formation of the caged radicals, assigned Q and QCO, and the free radicals,  $\text{Me}_3\text{C}$  and  $\text{Me}_3\text{CCO}$ , as two competing processes rather than two sequential steps (Appendix I). The photolyses of the azo and the ketone precursors can then be described by reactions (1) and (2) and (3) and (4), respectively. Although this is clearly an oversimplification of the systems, it does allow us to provide an adequate description of the photolysis and photo-oxidation of the two precursors.

### Photolysis of 2,2'-azoisobutane and 2,2,4,4-tetramethylpentan-3-one in the absence of oxygen

The caged *tert*-butyl radicals from the azo precursors can only undergo self-reaction, combination [reaction (5)] or disproportionation [reaction (6)]. Likewise, the caged radicals from the ketone either reform the parent ketone or yield 2-methylpropene and 2,2-dimethylpropanal [reaction (7)]. For the kinetic model the absolute rates of these reactions are unimportant, only the relative rates need to be considered. The rate of rotation of the radicals within the solvent cage is fast relative to cage reaction<sup>22</sup> and thus it can be assumed that, for the *tert*-butyl radicals in this model, the ratio of disproportionation to combination within the cage is identical to

that for free radical encounter pairs, since no orientation restrictions need be considered. Thus, as no distinction can be made between the products resulting from the cage reactions and those in the bulk solution, the cage effect may be thought to be unimportant. However, it does need to be considered because of the subsequent reaction of *tert*-butyl radicals with the solvent. If we assume (see above) that the caged radicals do not undergo reaction with oxygen in oxygenated solvents and, further, that they do not abstract hydrogen from the solvent, the observed excess of 2-methylpropane over 2-methylpropene in the oxygen-free experiments with both precursors, must arise from the abstraction of hydrogen from the solvent by free *tert*-butyl radicals. To find the rate constant for this abstraction reaction, a knowledge of the ratio of the rate of cage escape to cage reaction is needed.

In the presence of oxygen, the products from cage escape (oxygenated products) and cage reaction (hydrocarbons) are different and their relative yields can be used to calculate the required ratio of rate constants. This ratio is assumed to be constant for a given temperature in a particular solvent and thus can be used in the oxygen-free photolysis experiments.

When the ketone is being used, the free 2,2-dimethylpropanoyl radical, in the absence of any competing reaction, will decarbonylate [reaction (8)]. The rate constant for this reaction has been measured by Schuh *et al.*<sup>23</sup> who found  $\log(A_8/\text{dm}^3 \text{ mol}^{-1} \text{ s}^{-1}) = 11.9$  and  $E_8 = 38.9 \text{ kJ mol}^{-1}$ , in agreement with the rate constant obtained by Neville *et al.*<sup>24</sup> of  $7 \times 10^6 \text{ dm}^3 \text{ mol}^{-1} \text{ s}^{-1}$  at 298 K.

A choice of routes is available to the free *tert*-butyl radicals in both systems. Self-reaction leads to either combination [reaction (9)] or to disproportionation [reaction (10)]. These are reactions that have been extensively investigated<sup>19,25–28</sup> and for computer modelling in this study the values chosen were those obtained for their reaction in decane.

Free *tert*-butyl radicals may also abstract hydrogen from the solvent to form 2-methylpropane and a solvent radical, S [reaction (11)]. Decane has secondary hydrogen atoms in four different environments, but in this model no distinction is made between the different decyl radicals and their reactivities are assumed to be identical. The rates of abstraction of hydrogen from hydrocarbons by alkyl radicals are uncertain. Probably the most thorough study is that by Munger and Fischer<sup>29</sup> who examined the reaction of *tert*-butyl radicals with propan-2-ol. Although the rate constant for this reaction at a given temperature will be greater than that for reaction (11), it does provide an upper limit for the latter. Indeed, one of the aims of the photolysis experiments in the present study was to fix the rate parameters for reaction (11) as well as providing a comparison of our work with earlier results. The subsequent reactions of these solvent radicals are also required to complete the model [reactions (12)–(15)]. Although they are not well characterised they are believed to be diffusion-controlled and for the purpose of this work are given the same rate constants as those of the analogous *tert*-butyl reactions.

Thus of the rate constants needed to model the two photolyses, nine are known from the literature or can be predicted with a reasonable degree of accuracy. This leaves six that are unknown. Four are the photocleavages of the precursors [reactions (1)–(4)] and a fifth the abstraction of hydrogen from decane [reaction (11)]. As mentioned above the ratio of  $k_1 : k_2$  and  $k_3 : k_4$  can be calculated from the photo-oxidation studies, and the precise method of determining this ratio will be discussed in the next section. The total photolyses rates ( $k_1 + k_2$ ) and ( $k_3 + k_4$ ) can be calculated, to a first approximation, using the measured yields of products. These values were then adjusted to allow for the very small amount of *tert*-butyl 'lost' in the hydrocarbon produced in reaction (15). The absolute rate constant for the sixth unknown [reaction (7)] is kinetically not very important, but must be large enough to ensure than an implausible build-up of caged radicals does

not occur. The rate constants for reaction (11) were then adjusted to obtain a good comparison between experimental and simulated results.

It is very encouraging that there is a good correlation between the 'fitted' values of  $k_{11}$  obtained at the same temperatures for both the 2,2'-azoisobutane and the 2,2,4,4-tetramethylpentan-3-one systems (Appendix I) and the former compare well with values obtained for the reaction of *tert*-butyl radicals with propan-2-ol.<sup>29</sup>

To estimate the error in the derived values of  $k_{11}$  due to uncertainties in the other rate parameters, an error analysis was conducted on the value of  $k_{11}$  for the photolysis of the azo compound at 323 K (Fig. 3). Eleven reactions play a role in the mechanism [(1), (2), (5), (6), (9)–(15)]. The value for ( $k_1 + k_2$ ) is fitted for each experiment, so uncertainties in nine parameters ( $k_1/k_2$ ,  $k_5$ ,  $k_6$ ,  $k_9$ ,  $k_{10}$ ,  $k_{12}$ – $k_{15}$ ), could lead to an error in the estimated value of  $k_{11}$ . The ratio  $k_1/k_2$  derived from the ratio of unoxygenated/oxygenated products from Fig. 2 has a  $1\sigma$  value of  $\pm 5.30\%$ . Schuh and Fischer<sup>27</sup> quote an error band for  $k_9$  and  $k_{10}$  of  $\log(\Delta k) = \pm 0.4$  (assumed to be  $1\sigma$ ). The rate constants for the other reactions are assumed analogous to  $k_9$  and  $k_{10}$ , so were arbitrarily assumed to have approximately twice the uncertainty of  $\log(\Delta k) = \pm 0.7$ . Simulations were performed where the parameters were increased by their  $1\sigma$  value.  $k_{11}$  was then adjusted to give the measured excess of butane over butene. This gave a  $1\sigma$  for  $k_{11}$  of  $\pm 47\%$ , due predominantly to the sensitivity of  $k_{11}$  to the value of  $k_{10}$ .

As the temperature increases, the rate of formation of 2-methylpropane increases, reflecting the increasing rate constant of reaction (11). The relative decrease in the rate of formation of 2-methylpropene and 2,2,3,3-tetramethylbutane with temperature indicates the increased likelihood of cage escape. Both effects enhance the yield of 2-methylpropane compared to those of the other two hydrocarbons.

The Arrhenius parameters used in the simulations of the experiments with the azo compound and the ketone are listed together in Appendix I. Examples of the comparison with experimental data are given in Fig. 3 and 4.

#### Photo-oxidation of 2,2'-azoisobutane and 2,2,4,4-tetramethylpentan-3-one in decane

In the model, the photolyses of 2,2'-azoisobutane and 2,2,4,4-tetramethylpentan-3-one are again simplified to the two, one-step reactions (1) and (2) and reactions (3) and (4), respectively.

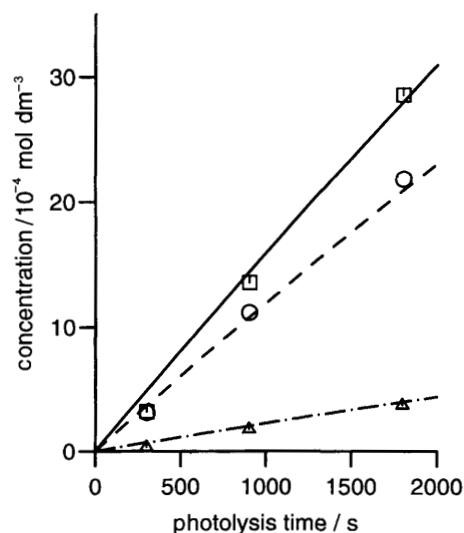
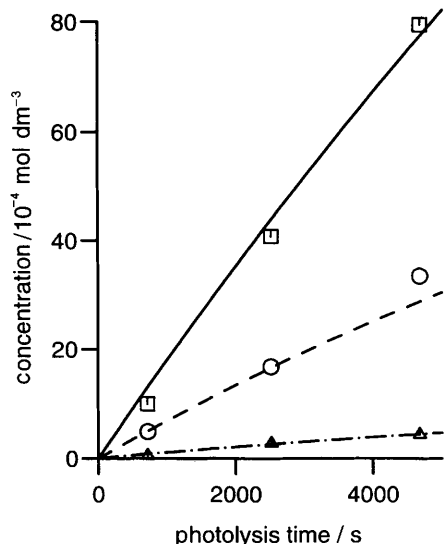


Fig. 3 Photolysis of 2,2'-azoisobutane in decane in a metal cell. Comparison of experimental and simulated data at 323 K. Azo compound  $2.7 \times 10^{-2} \text{ mol dm}^{-3}$ . See Fig. 1 for key.





**Fig. 4** Photolysis of 2,2,4,4-tetramethylpentan-3-one in a metal cell. Comparison of experimental and simulated data at 373 K. Ketone  $2.7 \times 10^{-2} \text{ mol dm}^{-3}$ . See Fig. 1 for key.

Whilst oxygen is still present in the solution of the azo precursor, the only route for the formation of hydrocarbon products involves the caged *tert*-butyl radicals. Therefore, using the total hydrocarbon product concentration during this initial period, the value of  $k_1$  can be calculated. To calculate the value of  $k_2$ , the total concentration of oxygenated products is needed. The concentration of *tert*-butanol can be used to calculate  $k_2$ , to a first approximation, but the value obtained has to be increased to allow for the formation of very small amounts of *tert*-butyl hydroperoxide and di-*tert*-butyl peroxide. Also, in the experiments where depletion of oxygen occurred, the final rate of production of hydrocarbons is determined by  $(k_1 + k_2)$  and thus  $k_2$  can be determined. A similar method has been used to determine  $k_3$  and  $k_4$ .

The caged radicals, as defined for this model, Q and QCO, are limited to self-reaction within the cage, reactions (5)–(7). For the azo system, reactions (9)–(34) are needed to describe the reactions of the radicals in the oxygenated bulk solution. In addition to these, reactions (8) and (35)–(47) are also required when the ketone is used as the precursor.

The reactions of alkyl radicals with oxygen [(e.g. reaction (16))] are thought to be diffusion controlled but there have been few measurements of their rate constants. Maillard *et al.*<sup>30</sup> give a rate constant of  $k_{16} = 4.93 \times 10^9 \text{ dm}^3 \text{ mol}^{-1} \text{ s}^{-1}$  for the reaction of *tert*-butyl radicals with oxygen in cyclohexane at 300 K. As the temperature dependence of this reaction has not been investigated, but will be small, and the exact value of  $k_{16}$  is kinetically unimportant for the modelling, this value was used across the temperature range studied. Other reactions of the free *tert*-butyl radicals are also unimportant whilst oxygen is present in solution, but their inclusion in the model is necessary to account for the products when the oxygen has been consumed.

In oxygenated solutions, the alkylperoxyl radical has a choice of two reaction pathways, hydrogen abstraction from the solvent, decane [reaction (17)] or reaction with another alkylperoxyl radical. Work on the autoxidation of decane leads to a value for the rate constant of  $3.8 \times 10^{-2} \text{ dm}^3 \text{ mol}^{-1} \text{ s}^{-1}$  per secondary hydrogen atom at 363 K for the abstraction of hydrogen from decane by a decylperoxyl radical.<sup>31</sup> This value is in good agreement with rate constants obtained for the reaction of *tert*-butylperoxyl radicals and similar hydrocarbons over a wide range of temperatures.<sup>32–35</sup> Combining these results leads to an *A*-factor of  $5.1 \times 10^{10}$

$\text{dm}^3 \text{ mol}^{-1} \text{ s}^{-1}$  and an activation energy of  $75.9 \text{ kJ mol}^{-1}$  which has been used to calculate the values of  $k_{17}$  in the present study.

The self-reaction of *tert*-butylperoxyl radicals has two possible pathways, which result in either the formation of di-*tert*-butyl peroxide [reaction (18)] or alkoxy radicals [reaction (19)]. Many studies have been performed, using a variety of techniques and precursors, to measure the rate constants for both the individual reactions and the total self-reaction rate constant ( $2k_t = 2k_{18} + 2k_{19}$ ).<sup>36,37</sup> Bennett, using UV spectroscopy, found a value of  $1.7 \times 10^4 \text{ dm}^3 \text{ mol}^{-1} \text{ s}^{-1}$  at 293 K in cyclohexane for the total self-reaction rate constant ( $2k_{18} + 2k_{19}$ ),<sup>38</sup> a value in good agreement with other recent measurements in both aqueous solution ( $2k_t = 2.0 \times 10^4 \text{ dm}^3 \text{ mol}^{-1} \text{ s}^{-1}$ ) using EPR spectroscopy<sup>39</sup> and in the gas phase ( $2k_t = 1.9 \times 10^4 \text{ dm}^3 \text{ mol}^{-1} \text{ s}^{-1}$ ) using molecular modulation spectroscopy.<sup>40</sup> The value obtained by Bennett for the total self-reaction rate constant has been used together with  $2k_{18} : 2k_{19}$  ratios obtained by product studies<sup>41</sup> to derive Arrhenius equations for  $2k_{18}$  and  $2k_{19}$ :  $2k_{18}/\text{dm}^3 \text{ mol}^{-1} \text{ s}^{-1} = 10^{9.6} \times \exp(-32.2/\text{kJ mol}^{-1})/RT$ ;  $2k_{19}/\text{dm}^3 \text{ mol}^{-1} \text{ s}^{-1} = 10^{10.8} \times \exp(-39.0/\text{kJ mol}^{-1})/RT$ .

The *tert*-butoxyl radicals produced in the self-reaction of two *tert*-butylperoxyl radicals can either abstract a hydrogen atom from a solvent molecule [reaction (20)] or undergo  $\beta$ -scission [reaction (21)], the latter reaction being very slow under the conditions used in the present study.<sup>42</sup> Few data for abstraction reactions with saturated hydrocarbons are available. Values of rate constants obtained with cyclopentane<sup>43,44</sup> and cyclohexane<sup>45</sup> were used to estimate  $\log(A_{20}/\text{dm}^3 \text{ mol}^{-1} \text{ s}^{-1}) = 9.0$  and  $E_{20} = 16.0 \text{ kJ mol}^{-1}$ .

The abstraction of hydrogen from the solvent, SH, by either *tert*-butoxyl or alkylperoxyl radicals results in the formation of a secondary alkyl radical, S. As with the *tert*-butyl radical, reactions (12)–(15) are included in the model to explain reactions that will occur once oxygen has been consumed. However, in the presence of oxygen, the radicals react by addition with oxygen to form secondary alkylperoxyl radicals,  $\text{SO}_2$ , [reaction (22)] and the rate constants have been assumed to be the same as reaction (16).

The predominant self-reaction for  $\text{SO}_2$ , being a secondary peroxyl, is by the Russell mechanism<sup>46</sup> [reaction (23)] at temperatures in this study. Smaller *et al.*<sup>47</sup> studying the autoxidation of decane by EPR spectroscopy obtained a value of  $3.0 \times 10^6 \text{ dm}^3 \text{ mol}^{-1} \text{ s}^{-1}$  for the self-reaction rate constant for decylperoxyl radicals at 298 K.

The  $\text{SO}_2$  radical can undergo a cross-reaction with *tert*-butylperoxyl radicals, [reaction (24)], which is important because it results in a faster overall rate of consumption of *tert*-butylperoxyl radicals than would be seen from self-reaction alone. Further, the ratio of  $[\text{ROH}] : [\text{ROOR}]$  will be enhanced if it occurs. Although this cross-reaction has not been studied directly, Fukuzumi and Oni<sup>48,49</sup> have found that the rate constant for the reaction between *tert*-butylperoxyl and  $\alpha$ -tetralylperoxyl radicals to be  $9.8 \times 10^4 \text{ dm}^3 \text{ mol}^{-1} \text{ s}^{-1}$  at 293 K whereas the value for the corresponding self-reaction of  $\alpha$ -tetralylperoxyl and *tert*-butyl radicals are  $1.5 \times 10^7$  and  $3.9 \times 10^2 \text{ dm}^3 \text{ mol}^{-1} \text{ s}^{-1}$ , respectively, at 293 K. This measured value compares well with the value of  $1.5 \times 10^5 \text{ dm}^3 \text{ mol}^{-1} \text{ s}^{-1}$  calculated using the cross-combination rule.

The abstraction of hydrogen by  $\text{SO}_2$  from the solvent [reaction (25)] results in the production of a secondary alkyl hydroperoxide,  $\text{SO}_2\text{H}$  and another S radical. No literature value is available for the rate of this reaction. The alternative intramolecular hydrogen abstraction of  $\text{SO}_2$  via a six-membered ring transition state to give a hydroperoxyalkyl radical is insignificant under the conditions used in this study.<sup>50</sup>

The secondary alkoxy radical, SO, can abstract hydrogen from the solvent [reaction (26)] and the same rate constant as

that of the corresponding *tert*-butoxyl reaction [reaction (20)] has been employed in this study.

The abstraction of hydrogen by both alkoxyl radicals from compounds other than the solvent has been investigated by simulation but the combination of the high reactivity of the radicals and the small concentration of all other compounds relative to the solvent means that these reactions are insignificant.

As the oxygen is depleted, other reactions of the alkyl radicals become important. In addition to the reactions encountered in the oxygen-free model, hydrogen abstraction reactions from some oxygenated products were considered. The experimentally observed decrease of *tert*-butyl hydroperoxide after oxygen depletion led to the inclusion of abstraction reactions by both *tert*-butyl and S [reactions (27) and (28)], and the corresponding abstraction reactions from  $\text{SO}_2\text{H}$  [reactions (29) and (30)]. Under these conditions, the concentration of alkyl radicals is relatively high and another reaction becomes important, one that yields dialkylperoxides [reactions (31)–(34)].

The stepwise photodecomposition of the ketone, which yields an acyl radical, plays a very important part in the reaction. In the early stages of the reaction the only hydrocarbon detected is 2-methylpropene; neither 2-methylpropane nor 2,2,3,3-tetramethylbutane are observed. Thus, as discussed above, one likely reaction between the caged 2,2-dimethylpropanoyl and *tert*-butyl radicals is disproportionation to yield 2-methylpropene and 2,2-dimethylpropanal [reaction (7)].<sup>20,51</sup> The fact that 2-methylpropene, without 2-methylpropane, was detected initially suggests that the reaction does indeed occur. However, the absence of any aldehyde in the product studies implies that it is rapidly removed. Preliminary simulations were performed with all radicals abstracting the aldehydic hydrogen, but by limiting the rate constants to reasonable values no effective reduction of the aldehyde yield was observed. Thus it was concluded that the aldehyde must also be photolysed at such a rate as to remove it effectively [reaction (35)]. The formyl radical formed reacts very rapidly in oxygen [reaction (36)], the resulting hydroperoxyl radical having a variety of available reaction pathways, including abstraction of hydrogen from the solvent [reaction (37)] and reaction with other peroxy radicals [reactions (38)–(40)].

Thus reactions (35)–(47) were included in the overall model to account for reactions subsequent to the formation of 2,2-dimethylpropanal, produced in a solvent cage [reaction (7)] and the rate constants chosen were from the literature or from closely analogous reactions.

Increasing the temperature of the system leads to changes in the product distributions both before and after oxygen depletion. Thus, in the initial phase the lower concentration of oxygen and the increased rate of cage escape at higher temperatures account for the lower yield of oxygenates and of 2-methylpropene, respectively. Following oxygen consumption, as discussed above, increased temperature not only favours cage escape but also hydrogen abstraction from the solvent [reaction (11)] over dimerisation and disproportionation [reactions (9) and (10)] of the *tert*-butyl radicals leading to an increased rate of formation of 2-methylpropane relative to 2-methylpropene and 2,2,3,3-tetramethylbutane.

The rate constants for the reactions in this model are listed in Appendix I and the examples of the results obtained from the computer simulations are compared with the experimental data in Figs 1–8.

## Conclusions

A unified mechanism is presented to account for the reactions of *tert*-butylperoxyl and related radicals in a hydrocarbon solvent, using two different precursors, 2,2'-azoisobutane and 2,2,4,4-tetramethylpentan-3-one. Using known or best esti-

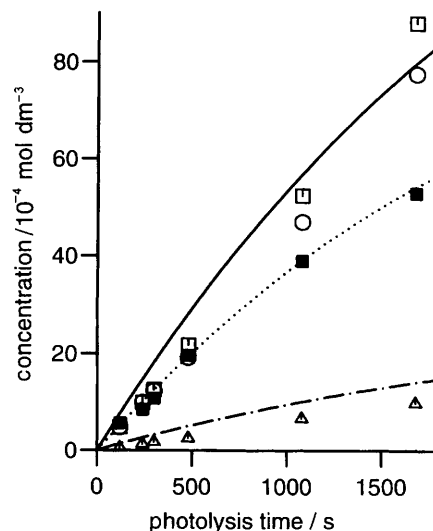


**Fig. 5** Photo-oxidation of 2,2'-azoisobutane in a glass cell. Comparison of experimental and simulated data at 298 K. Azo compound  $2.7 \times 10^{-2} \text{ mol dm}^{-3}$ ; oxygen  $6.1 \times 10^{-3} \text{ mol dm}^{-3}$ . See Fig. 1 for key.

mates of the rate constants for the individual steps, the time-dependent product distributions from both precursors, under varying conditions, have been effectively modelled by computer simulation. The change of conditions include two different reactors, a wide temperature range and the presence and absence of oxygen.

The key to understanding these processes has been to distinguish between the reactions of the germinate pair of radicals formed by photolysis within a solvent cage and those that occur in the bulk of solution. This has been achieved with oxygen-saturated solutions by assuming that radicals that escape the solvent cage are all trapped by oxygen whereas those that remain inside the solvent cage are not. This interpretation also accounts for the difference in the product distributions of gas and solution phase photo-oxidations since the former do not involve a solvent cage.

Decisions underlying the choice of the magnitude of the rate constants used in the reaction scheme have been discussed above, reaction by reaction. To summarise, the key

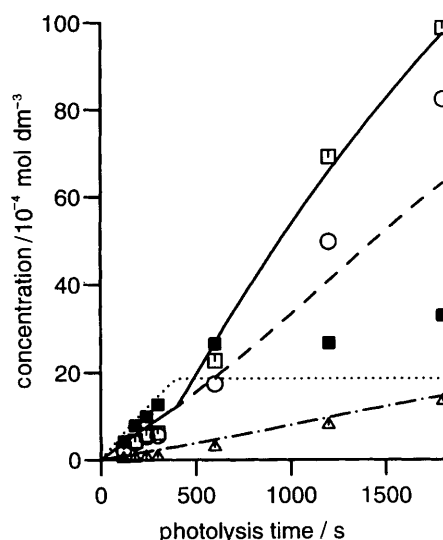


**Fig. 6** Photo-oxidation of 2,2'-azoisobutane in a glass cell. Comparison of experimental and simulated data at 348 K. Azo compound  $2.7 \times 10^{-2} \text{ mol dm}^{-3}$ ; oxygen  $4.8 \times 10^{-3} \text{ mol dm}^{-3}$ . See Fig. 1 for key.



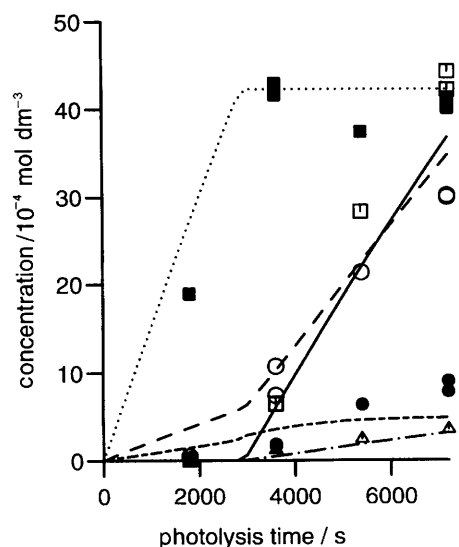


**Fig. 7** Photo-oxidation of 2,2,4,4-tetramethylpentan-3-one in a glass cell. Comparison of experimental and simulated data at 298 K. Ketone  $2.7 \times 10^{-2} \text{ mol dm}^{-3}$ ; oxygen  $6.1 \times 10^{-3} \text{ mol dm}^{-3}$ . See Fig. 1 for key.

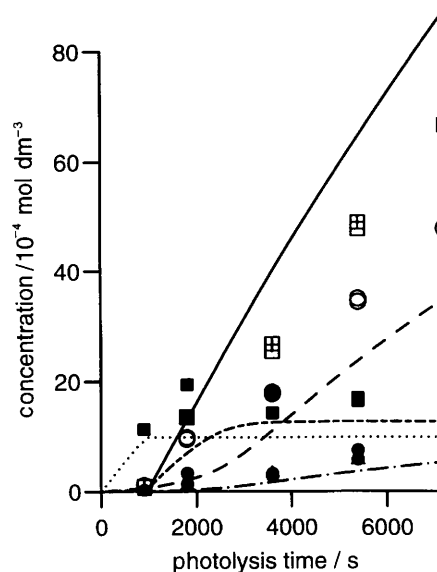


**Fig. 8** Photo-oxidation of 2,2,4,4-tetramethylpentan-3-one in a metal cell. Comparison of experimental and simulated data at 348 K. Ketone  $2.7 \times 10^{-2} \text{ mol dm}^{-3}$ ; oxygen  $4.8 \times 10^{-3} \text{ mol dm}^{-3}$ . See Fig. 1 for key.

reactions involving *tert*-butyl and radicals derived from it are reactions (1)–(11), (13)–(21), (27) and (29). The relative rates of initiation (1) and (2) for the azo precursor and (3) and (4) for the ketone, are of paramount importance for describing the relative appearance of oxygenated and hydrocarbon products. They are obtained by fitting, but are self-consistent. Relative rate constants for reactions (5)–(7) and for (9), (10) are needed but they are well documented. The rates of reactions (8), (13)–(15) and (16) and of later reactions are not kinetically sensitive within the parameters described, *i.e.* within the errors given in the literature.

A feature of some of the photo-oxidations, in particular those at higher temperatures, where the concentrations of oxygen in decane are lower, is the near or complete consumption of oxygen during reaction. The kinetic model accommodates this depletion of oxygen and accounts for the marked change in product distribution, an increase in hydrocarbons at the expense of oxygenates, that results. Other more subtle product changes that occur when the oxygen is consumed including a decrease in the yield of *tert*-butyl hydroperoxide and an increase in di-*tert*-butyl peroxide, are also predicted by

the model as a result of the increase in the concentration of alkyl radicals in the anaerobic solutions.

The solvent not only influences the reactions through the cage reactions described above but also through its reactions with the *tert*-butyl, *tert*-butylperoxyl and *tert*-butoxyl radicals. In the oxygen-free photolysis of 2,2'-azoisobutane the greater yield of isobutane over isobutene arises from hydrogen abstraction from the solvent by cage-escaped *tert*-butyl radicals since disproportionation of these radicals in the solvent cage leads to equal yields of alkene and alkane. In photo-oxidations, oxygen accounts reveal a large shortfall in the measured yields of oxygenated products. The missing oxygen ends up as solvent oxidation products, decanols and decanones. Indeed the simulation of the results with the kinetic model requires inclusion of the reactions of  $\text{SO}_2$  and  $\text{SO}$  radical.

We thank John Pragnell and Dr Andrew Markson, of Castrol International, for helpful discussions and their company for generous financial support throughout this study.

#### Appendix I Reaction mechanism for the photolysis and photo-oxidation of 2,2'-azoisobutane and 2,2,4,4-tetramethylpentan-3-one [ $k = A \exp(-E_a/RT)$ ]

		$A/\text{dm}^3 \text{ mol}^{-1} \text{ s}^{-1}$	$E_a/\text{kJ mol}^{-1}$	
<b>initiation</b>				
(1)	$\text{Me}_3\text{CN}_2\text{CMe}_3 \xrightarrow{h\nu} \text{Q} + \text{Q} + \text{N}_2$			note 1
(2)	$\text{Me}_3\text{CN}_2\text{CMe}_3 \xrightarrow{h\nu} \text{Me}_3\text{C} + \text{Me}_3\text{C} + \text{N}_2$			note 1
(3)	$\text{Me}_3\text{CCOCMe}_3 \xrightarrow{h\nu} \text{Q} + \text{QCO}$			note 1
(4)	$\text{Me}_3\text{CCOCMe}_3 \xrightarrow{h\nu} \text{Me}_3\text{C} + \text{Me}_3\text{CCO}$			note 1
<b>cage reactions</b>				
(5)	$\text{Q} + \text{Q} \longrightarrow \text{C}_8\text{H}_{18}$	$2.11 \times 10^{11}$	15.3	as reaction (9), note 2
(6)	$\text{Q} + \text{Q} \longrightarrow \text{C}_4\text{H}_{10} + \text{C}_4\text{H}_8$	$1.31 \times 10^{11}$	9.83	as reaction (10), note 2
(7)	$\text{QCO} + \text{Q} \longrightarrow \text{C}_4\text{H}_8 + \text{Me}_3\text{CCHO}$	$1.00 \times 10^{10}$	0	note 3
<b>radical reactions in the absence of oxygen</b>				
(8)	$\text{Me}_3\text{CCO} \longrightarrow \text{Me}_3\text{C} + \text{CO}$	$7.94 \times 10^{11}$	38.9	ref. 24
(9)	$\text{Me}_3\text{C} + \text{Me}_3\text{C} \longrightarrow \text{C}_8\text{H}_{18}$	$2.11 \times 10^{11}$	15.3	note 4
(10)	$\text{Me}_3\text{C} + \text{Me}_3\text{C} \longrightarrow \text{C}_4\text{H}_{10} + \text{C}_4\text{H}_8$	$1.31 \times 10^{11}$	9.83	note 4

Appendix I (continued)

			$A^a/\text{dm}^3 \text{ mol}^{-1} \text{ s}^{-1}$	$E_a/\text{kJ mol}^{-1}$	
(11)	$\text{Me}_3\text{C} + \text{SH}$	$\longrightarrow \text{C}_4\text{H}_{10} + \text{S}$			note 5
(12)	$\text{S} + \text{S}$	$\longrightarrow \text{non-radical products}$	$2.11 \times 10^{11}$	15.3	as reaction (9)
(13)	$\text{S} + \text{Me}_3\text{C}$	$\longrightarrow \text{C}_4\text{H}_8 + \text{SH}$	$6.55 \times 10^{10}$	9.83	as reaction (10)
(14)	$\text{S} + \text{Me}_3\text{C}$	$\longrightarrow \text{C}_4\text{H}_{10} + \text{S}(-\text{H})$	$6.55 \times 10^{10}$	9.83	as reaction (10)
(15)	$\text{S} + \text{Me}_3\text{C}$	$\longrightarrow \text{C}_{14}\text{H}_{30}$	$2.11 \times 10^{11}$	15.3	as reaction (9)
radical reactions in the presence of oxygen					
(16)	$\text{Me}_3\text{C} + \text{O}_2$	$\longrightarrow \text{Me}_3\text{CO}_2$	$4.93 \times 10^9$	0	ref. 30
(17)	$\text{Me}_3\text{CO}_2 + \text{SH}$	$\longrightarrow \text{Me}_3\text{CO}_2\text{H} + \text{S}$	$5.06 \times 10^{10}$	75.9	ref. 31–35
(18)	$\text{Me}_3\text{CO}_2 + \text{Me}_3\text{CO}_2$	$\longrightarrow \text{Me}_3\text{CO}_2\text{CMe}_3 + \text{O}_2$	$7.92 \times 10^8$	32.2	ref. 38, 39, 41
(19)	$\text{Me}_3\text{CO}_2 + \text{Me}_3\text{CO}_2$	$\longrightarrow \text{Me}_3\text{CO} + \text{Me}_3\text{CO} + \text{O}_2$	$6.29 \times 10^{10}$	39.0	ref. 38, 39, 41
(20)	$\text{Me}_3\text{CO} + \text{SH}$	$\longrightarrow \text{Me}_3\text{COH} + \text{S}$	$1.00 \times 10^9$	16.0	ref. 43, 44, 45
(21)	$\text{Me}_3\text{CO}$	$\longrightarrow \text{Me} + \text{Me}_2\text{CO}$	$9.60 \times 10^{14}$	63.4	ref. 42
(22)	$\text{S} + \text{O}_2$	$\longrightarrow \text{SO}_2$	$4.93 \times 10^9$	0	as reaction (16)
(23)	$\text{SO}_2 + \text{SO}_2$	$\longrightarrow \text{SOH} + \text{S}(-\text{H})=\text{O} + \text{O}_2$	$3.00 \times 10^6$	0	ref. 47
(24)	$\text{SO}_2 + \text{Me}_3\text{CO}_2$	$\longrightarrow \text{S}(-\text{H})=\text{O} + \text{Me}_3\text{COH} + \text{O}_2$	$9.75 \times 10^7$	16.1	note 6
(25)	$\text{SO}_2 + \text{SH}$	$\longrightarrow \text{SO}_2\text{H} + \text{S}$	$5.06 \times 10^{10}$	75.9	as reaction (17)
(26)	$\text{SO} + \text{SH}$	$\longrightarrow \text{SOH} + \text{S}$	$1.00 \times 10^9$	16.0	as reaction (20)
(27)	$\text{Me}_3\text{C} + \text{Me}_3\text{CO}_2\text{H}$	$\longrightarrow \text{C}_4\text{H}_{10} + \text{Me}_3\text{CO}_2$	$5.00 \times 10^8$	23.5	note 7
(28)	$\text{S} + \text{Me}_3\text{CO}_2\text{H}$	$\longrightarrow \text{SH} + \text{Me}_3\text{CO}_2$	$5.00 \times 10^8$	23.5	as reaction (27)
(29)	$\text{Me}_3\text{C} + \text{SO}_2\text{H}$	$\longrightarrow \text{C}_4\text{H}_{10} + \text{SO}_2$	$5.00 \times 10^8$	23.5	as reaction (27)
(30)	$\text{S} + \text{SO}_2\text{H}$	$\longrightarrow \text{SH} + \text{SO}_2$	$5.00 \times 10^8$	23.5	as reaction (27)
(31)	$\text{Me}_3\text{C} + \text{Me}_3\text{CO}_2$	$\longrightarrow \text{Me}_3\text{COOCMe}_3$	$1.00 \times 10^{10}$	0	note 3
(32)	$\text{Me}_3\text{C} + \text{SO}_2$	$\longrightarrow \text{SOOCMe}_3$	$1.00 \times 10^{10}$	0	as reaction (31)
(33)	$\text{S} + \text{Me}_3\text{CO}_2$	$\longrightarrow \text{SOOCMe}_3$	$1.00 \times 10^{10}$	0	as reaction (31)
(34)	$\text{S} + \text{SO}_2$	$\longrightarrow \text{SOOS}$	$1.00 \times 10^{10}$	0	as reaction (31)
photo-oxidation reactions of 2,2-dimethylpropanal					
(35)	$\text{Me}_3\text{CCHO}$	$\xrightarrow{h\nu} \text{HCO} + \text{Me}_3\text{C}$	$5.20 \times 10^{-4}$	0	note 3
(36)	$\text{HCO} + \text{O}_2$	$\longrightarrow \text{HO}_2 + \text{CO}$	$3.00 \times 10^9$	0	ref. 17
(37)	$\text{HO}_2 + \text{SH}$	$\longrightarrow \text{H}_2\text{O}_2 + \text{S}$	$5.06 \times 10^{10}$	75.9	as reaction (17)
(38)	$\text{HO}_2 + \text{HO}_2$	$\longrightarrow \text{H}_2\text{O}_2 + \text{O}_2$	$1.80 \times 10^9$	0	ref. 52
(39)	$\text{HO}_2 + \text{Me}_3\text{CO}_2$	$\longrightarrow \text{Me}_3\text{CO}_2\text{H} + \text{O}_2$	$2.39 \times 10^9$	16.1	note 6
(40)	$\text{HO}_2 + \text{SO}_2$	$\longrightarrow \text{SO}_2\text{H} + \text{O}_2$	$1.47 \times 10^8$	0	note 6
(41)	$\text{Me}_3\text{CCO} + \text{O}_2$	$\longrightarrow \text{Me}_3\text{CCO}_3$	$4.93 \times 10^9$	0	as reaction (16)
(42)	$\text{Me}_3\text{CCO}_3 + \text{SH}$	$\longrightarrow \text{Me}_3\text{CCO}_3\text{H} + \text{S}$	$5.06 \times 10^{10}$	75.9	as reaction (17)
(43)	$\text{Me}_3\text{CCO}_3 + \text{Me}_3\text{CCO}_3$	$\longrightarrow \text{Me}_3\text{CCO}_2 + \text{Me}_3\text{CCO}_2 + \text{O}_2$	$6.30 \times 10^6$	0	ref. 53
(44)	$\text{MeCCO}_2$	$\longrightarrow \text{Me}_3\text{C} + \text{CO}_2$	$1.00 \times 10^{11}$	0	note 3
(45)	$\text{Me}_3\text{CCO}_3 + \text{SO}_2$	$\longrightarrow \text{Me}_3\text{CCO}_2 + \text{SO} + \text{O}_2$	$3.45 \times 10^8$	10.7	note 6
(46)	$\text{Me}_3\text{CCO}_3 + \text{Me}_3\text{CO}_2$	$\longrightarrow \text{Me}_3\text{CCO}_2 + \text{Me}_3\text{CO} + \text{O}_2$	$1.26 \times 10^9$	19.5	note 6
(47)	$\text{Me}_3\text{CCO}_3 + \text{HO}_2$	$\longrightarrow \text{Me}_3\text{CCO}_3\text{H} + \text{O}_2$	$2.13 \times 10^8$	0	note 6

<sup>a</sup> Except for reactions (8), (21) and (35) where the units are s<sup>-1</sup>.

1. The overall photolysis rate for the azo and ketone reactants [(*k*<sub>1</sub> + *k*<sub>2</sub>) and (*k*<sub>3</sub> + *k*<sub>4</sub>)] were adjusted for each simulation to give agreement between the measured and predicted concentrations for the sum of the observed species. The ratios of caged to uncaged photolysis (*k*<sub>1</sub>/*k*<sub>2</sub> and *k*<sub>3</sub>/*k*<sub>4</sub>) were adjusted to give agreement between measured and simulated ratios of *tert*-C<sub>4</sub>H<sub>9</sub>OH/hydrocarbons for photo-oxidation experiments, while oxygen was present. The photolysis rate constants used were:

azo photolysis			ketone photolysis		
Fig.	<i>k</i> <sub>1</sub> /s	<i>k</i> <sub>2</sub> /s	Fig.	<i>k</i> <sub>3</sub> /s	<i>k</i> <sub>4</sub> /s
2	$6.84 \times 10^{-5}$	$4.20 \times 10^{-5}$	1	$8.76 \times 10^{-6}$	$7.47 \times 10^{-5}$
3	$3.91 \times 10^{-5}$	$2.40 \times 10^{-5}$	4	$7.20 \times 10^{-7}$	$5.40 \times 10^{-5}$
5	$2.80 \times 10^{-5}$	$9.89 \times 10^{-5}$	7	$8.00 \times 10^{-6}$	$3.29 \times 10^{-5}$
6	$1.50 \times 10^{-4}$	$1.94 \times 10^{-4}$	8	$2.50 \times 10^{-6}$	$5.50 \times 10^{-5}$

2. The rate constants used for self reactions are defined by the rate equations:  $d[\text{R}]/dt = -2k[\text{R}]^2$ .
3. Estimate.
4. The rate constants for *k*<sub>9</sub> and *k*<sub>10</sub>, have been derived from the values quoted by Schuh and Fischer<sup>27</sup> of  $2(k_9 + k_{10}) = 4.47 \times 10^{11} \exp[-10.8 \text{ kJ (mol RT)}^{-1}] \text{ dm}^3 \text{ mol}^{-1} \text{ s}^{-1}$  and  $k_{10}/k_9 = 0.62 \exp[-5.5 \text{ kJ (mol RT)}^{-1}]$ .
5. The rate constant for *k*<sub>11</sub> was determined by adjusting its value to obtain a good fit between the measured and predicted ratio of C<sub>4</sub>H<sub>10</sub>/C<sub>4</sub>H<sub>8</sub> for the photolysis experiments.

temperature /K	<i>k</i> <sub>11</sub> (azo) /dm <sup>3</sup> mol <sup>-1</sup> s <sup>-1</sup>	<i>k</i> <sub>11</sub> (ketone) /dm <sup>3</sup> mol <sup>-1</sup> s <sup>-1</sup>
323	9.5	7.0
348	8.5	11.5
373	—	26.0

6. The rates for radical–radical cross-reactions have been estimated by using the cross-combination rule.
7. *k*<sub>27</sub> was determined by adjusting its value to obtain a good fit between the experimental and simulated rate of build up of di-*tert*-butyl peroxide.

## References

- 1 See e.g. A. Hubmann and A. Lanik, *Tribologie Schmierungstech.*, 1985, **35**, 138; R. K. Jensen, S. Korcek, M. Zinbo and M. D. Johnson, *Int. J. Chem. Kinet.*, 1990, **22**, 1095; S. Blaine and P. E. Savage, *Ind. Eng. Chem. Res.*, 1991, **30**, 792; 1991, **30**, 2185.
- 2 J. E. Bennett, G. Brunton, J. R. Lindsay Smith, T. M. F. Salmon and D. J. Waddington, *J. Chem. Soc., Faraday Trans. 1*, 1987, **83**, 2421.
- 3 J. E. Bennett, G. Brunton, J. R. Lindsay Smith, T. M. F. Salmon and D. J. Waddington, *J. Chem. Soc., Faraday Trans. 1*, 1987, **83**, 2433.
- 4 R. Ohme, H. Preuschhof and H. U. Heyne, *Organic Synthesis*, 1972, **52**, 11.
- 5 J. W. Timberlake, M. L. Hodges and K. Betterton, *Synthesis*, 1972, 632.
- 6 C. F. Cullis and E. J. Newitt, *Proc. R. Soc. London, Ser. A*, 1956, **237**, 530.
- 7 T. J. Kelly, P. H. Daun and S. E. Schwartz, *J. Geophys. Res.*, 1985, **90**, 7861.
- 8 M. J. Brown, D. Phil. Thesis, University of York, 1984.
- 9 T. Nash, *J. Biochem.*, 1953, **55**, 416.
- 10 T. M. F. Salmon, D. Phil. Thesis, University of York, 1988.
- 11 A. Woolley, D. Phil. Thesis, University of York, 1980.
- 12 P. M. Patwardhan, MSc Thesis, University of York, 1986.
- 13 L. J. Kirsch, D. A. Parkes, D. J. Waddington and A. Woolley, *J. Chem. Soc., Faraday Trans. 1*, 1978, **74**, 2293.
- 14 L. J. Kirsch, D. A. Parkes, D. J. Waddington and A. Woolley, *J. Chem. Soc., Faraday Trans. 1*, 1979, **75**, 2678.
- 15 L. T. Cowley, D. J. Waddington and A. Woolley, *J. Chem. Soc., Faraday Trans. 1*, 1982, **78**, 2535.
- 16 P. S. Engel, *Chem. Rev.*, 1980, **80**, 99.
- 17 D. L. Baulch, C. J. Cobos, R. A. Cox, C. Esser, P. Frank, Th. Just, J. A. Kerr, M. J. Pilling, J. Troe, R. W. Walker and J. Warnatz, *J. Phys. Chem. Ref. Data*, 1992, **21**, 411.
- 18 G. S. Hammond, C-H. S. Wu, O. D. Trap, J. Warkentin and R. T. Keys, *J. Am. Chem. Soc.*, 1960, **82**, 5394.
- 19 H. H. Schuh and H. Fischer, *Helv. Chim. Acta*, 1978, **61**, 2130.
- 20 E. B. Abuin, M. V. Encinas, S. Diaz and E. A. Lissi, *Int. J. Chem. Kinet.*, 1984, **16**, 503.
- 21 W. B. Moniz, C. F. Poranski Jr. and S. A. Sojka, *J. Org. Chem.*, 1975, **40**, 2946.
- 22 F. D. Greene, M. A. Berwick and J. C. Stowell, *J. Am. Chem. Soc.*, 1970, **92**, 867.
- 23 H. Schuh, E. S. Hamilton Jr., H. Paul and H. Fischer, *Helv. Chim. Acta*, 1974, **57**, 2011.
- 24 A. G. Neville, C. E. Brown, D. M. Rayner, J. Lusztyk and K. U. Ingold, *J. Am. Chem. Soc.*, 1991, **113**, 1869.
- 25 S. A. Weiner and G. S. Hammond, *J. Am. Chem. Soc.*, 1969, **91**, 986.
- 26 J. E. Bennett and R. Summers, *J. Chem. Soc., Perkin Trans. 2*, 1977, 1504.
- 27 H. H. Schuh and H. Fischer, *Int. J. Chem. Kinet.*, 1976, **8**, 341.
- 28 H. H. Schuh and H. Fischer, *Helv. Chim. Acta*, 1978, **61**, 2462.
- 29 K. Munger and H. Fischer, *Int. J. Chem. Kinet.*, 1984, **16**, 1213.
- 30 B. Maillard, K. U. Ingold and J. C. Scaiano, *J. Am. Chem. Soc.*, 1983, **105**, 5095.
- 31 E. Niki and Y. Kamiya, *Bull. Chem. Soc. Jpn.*, 1975, **48**, 3226.
- 32 S. Korcek, J. H. B. Chenier, J. A. Howard and K. U. Ingold, *Can. J. Chem.*, 1972, **50**, 2285.
- 33 J. H. B. Chenier, S. B. Tong and J. A. Howard, *Can. J. Chem.*, 1978, **56**, 3047.
- 34 J. A. Howard and J. H. B. Chenier, *Can. J. Chem.*, 1980, **58**, 2808.
- 35 J. A. Howard, J. H. B. Chenier and D. A. Holden, *Can. J. Chem.*, 1978, **56**, 170.
- 36 P. Neta, R. E. Huie and A. B. Ross, *J. Phys. Chem. Ref. Data*, 1990, **19**, 413.
- 37 J. A. Howard and J. C. Scaiano, in *Landolt-Burnstein's Radical Reaction Rates in Liquids*, ed. H. Fischer, Springer-Verlag, Berlin, 1984, vol. 13d.
- 38 J. E. Bennett, *J. Chem. Soc., Faraday Trans. 1*, 1987, **83**, 1805.
- 39 J. E. Bennett, *J. Chem. Soc., Faraday Trans.*, 1990, **86**, 3247.
- 40 L. J. Kirsch and D. A. Parkes, *Fifth Int. Symp. Gas Kinetics*, Manchester 1977, The Chemical Society Gas Kinetics Group, paper 37.
- 41 J. A. Howard and K. U. Ingold, *J. Am. Chem. Soc.*, 1968, **90**, 1058.
- 42 K. Fuke, A. Hasegawa, M. Uede and M. Itoh, *Chem. Phys. Lett.*, 1981, **84**, 176.
- 43 H. Paul, R. D. Small Jr. and J. C. Scaiano, *J. Am. Chem. Soc.*, 1978, **100**, 4520.
- 44 S. K. Wong, *Int. J. Chem. Kinet.*, 1981, **13**, 413.
- 45 J. A. Howard and J. C. Scaiano, unpublished results.
- 46 G. A. Russell, *J. Am. Chem. Soc.*, 1957, **79**, 3871.
- 47 B. Smaller, J. R. Remko and E. C. Avery, *J. Chem. Phys.*, 1968, **48**, 5174.
- 48 S. Fukuzumi and Y. J. Ono, *J. Phys. Chem.*, 1976, **80**, 2973.
- 49 S. Fukuzumi and Y. J. Ono, *J. Phys. Chem.*, 1977, **81**, 1985.
- 50 N. L. Arthur and J. R. Christien, *Int. J. Chem. Kinet.*, 1987, **19**, 261.
- 51 R. C. Neuman Jr. and M. E. Frink, *J. Org. Chem.*, 1983, **48**, 2430.
- 52 J. A. Howard and K. U. Ingold, *Can. J. Chem.*, 1967, **45**, 785.
- 53 G. E. Zaikov, J. A. Howard and K. U. Ingold, *Can. J. Chem.*, 1969, **47**, 3017.

Paper 6/03283D; Received 10th May, 1996